Phase behaviour of argon and krypton adsorbed in mesoporous Vycor glass

2003 J. Phys.: Condens. Matter 15 4709

(http://iopscience.iop.org/0953-8984/15/27/305)

INSTITUTE OF PHYSICS PUBLISHING JOURNAL OF PHYSICS: CONDENSED MATTER

J. Phys.: Condens. Matter **15** (2003) 4709–4715 PII: S0953-8984(03)61948-X

Phase behaviour of argon and krypton adsorbed in mesoporous Vycor glass

D G Jones and H M Fretwell

Department of Physics, University of Wales Swansea, Singleton Park, Swansea SA2 8PP, UK

E-mail: h.m.fretwell@swan.ac.uk

Received 9 April 2003
Published 27 June 2003
Online at stacks.iop.org/JPhysCM/15/4709

Abstract

The phase behaviour of Ar and Kr adsorbed in Vycor glass at pressures and temperatures above the bulk triple point and below the bulk critical point has been investigated. Ar is found to condense in the pores ∼2 K above the bulk transition and freeze ∼10 K below the bulk transition. In contrast the condensation transition for Kr is shifted up by 4 K and freezing shifted down by 15 K. There is a pronounced hysteresis (4–6 K) at the liquid/solid phase boundary and a lesser amount (∼2 K) at the gas/liquid boundary. We find clear differences between the pore filling and emptying processes at the gas/liquid phase boundary and evidence of pore blocking on desorption. In addition microbubbles or large gas–liquid interfaces are thought to occur when Kr condenses in the pores but this effect is absent in Ar. Finally, solid Ar in the pores melts in a more continuous way than Kr.

1. Introduction

When fluids are adsorbed in narrow pores just a few nanometres wide, such as those found in Vycor glass [1] and zeolite, there is often a dramatic change in the phase behaviour of the fluid [2–5]. Capillary forces, the finite size and disorder associated with the medium often result in shifted phase transitions and hysteresis. In general one observes a shift in the gas–liquid transition toward higher temperatures and a more pronounced depression of the freezing point to lower temperatures. Hysteresis at the liquid/solid phase boundary is often larger than that seen at the gas–liquid boundary.

Although these general observations above are now relatively well established, there is much to be learned about the nature of the transitions and of the fluid in the pore. There have been a few experimental studies [6] of the phase behaviour of pure Ar and/or Kr gases in Vycor and other porous media. In this paper we report on positron annihilation studies of the phase behaviour of argon and krypton adsorbed in mesoporous Vycor glass at pressures above the bulk triple point and below the bulk critical point. These gases were chosen for

the comparatively simple nature of their interatomic forces and the easy accessibility of the relevant phase boundaries. In addition to the Doppler broadening positron annihilation method presented in this paper, many other techniques (including vapour pressure measurement, x-ray diffraction analysis and small-angle neutron scattering investigation) have been employed by researchers; see e.g. [7, 8]. The positron annihilation method is complementary to these other techniques and benefits from the tendency of the positron to seek out and annihilate from less dense regions such as the pores in Vycor glass.

2. Positrons and positronium in porous glass

When energetic ($<$0.5 MeV) positrons from a ^{22}Na radioisotope enter a porous glass sample they rapidly thermalize in the glass matrix. Thermalized positrons may then annihilate as free positrons in the glass matrix or migrate to the pores and form a bound electron–positron state known as positronium (Ps) [9]. Ps can exist in two forms. In vacuum, the relatively long-lived ($\sim$140 ns) ortho-positronium (oPs) (parallel electron–positron spins) decays via the emission of 3γ photons. Para-positronium (pPs) (anti-parallel spins) has a considerably shorter lifetime of $\sim$125 ps and annihilates via 2γ photons. In a mesopore (pore radius less than oPs mean free path) a thermalized oPs will undergo a large number of collisions with the pore walls during its long lifetime. This may result in the positron annihilating with an electron of opposite spin from the pore wall. In this situation the oPs is said to be 'quenched' and two γs are produced instead of three. When the pores are filled with gas, the gas molecules contribute to the quenching and the 2γ annihilation contribution is increased. A substantial increase in quenching and consequent 2γ contribution will occur when the fluid condenses in the pores, due to the increase in fluid density. Similar effects are to be expected at gas $\rightarrow$ solid and, perhaps to a lesser extent, at liquid $\rightarrow$ solid transitions. In addition, when the fluid solidifies, Ps formation may be 'inhibited' as it is less likely to form in a rigid solid structure compared to, for example, the liquid state where it can exist inside a bubble [10]. In liquid Ar for example, the balance between the zero-point pressure of the Ps atom and the surface tension of the liquid leads to a bubble diameter of $\sim$15 Å [11]. Thus, by monitoring the $3\gamma/2\gamma$ annihilation ratio we have a novel way of probing the phase behaviour under varying conditions of temperature and pressure.

3. Experimental details

The experiments were performed in a small pressure cell with free access to an external gas reservoir via a narrow stainless steel capillary tube. The temperature of the cell was monitored via a thermocouple and a Pt sensor and the pressure controlled via an external gas handling system. The porous samples were commercially available Vycor glass containing interconnecting cylindrical pores, occupying $\sim$30% of the total volume of the glass [1]. AFM measurements on the samples showed that they had pore diameters in the range $\sim$3–7 nm. Two identical samples were sandwiched around a positron source of $\sim$20 μCi ^{22}Na, deposited on $\sim$8 μm Kapton foil, and the whole assembly inserted in to the cell. A small gap (a few microns wide) was created between the source and the samples, which, as has been shown in the case of CO_2 in Vycor [9], permits the simultaneous measurement of the bulk phase transitions. The relative strength of the bulk and pore signals can be adjusted by altering the size of this gap, but due to the geometry of the positron source, it is difficult to totally remove the bulk signal. Nevertheless it provides a very useful check on the temperature calibration of the system. The gases investigated were Ar (99.998% purity) and Kr (99.995% purity). Isobaric experiments were performed to locate the phase boundaries and further scanning isothermal experiments

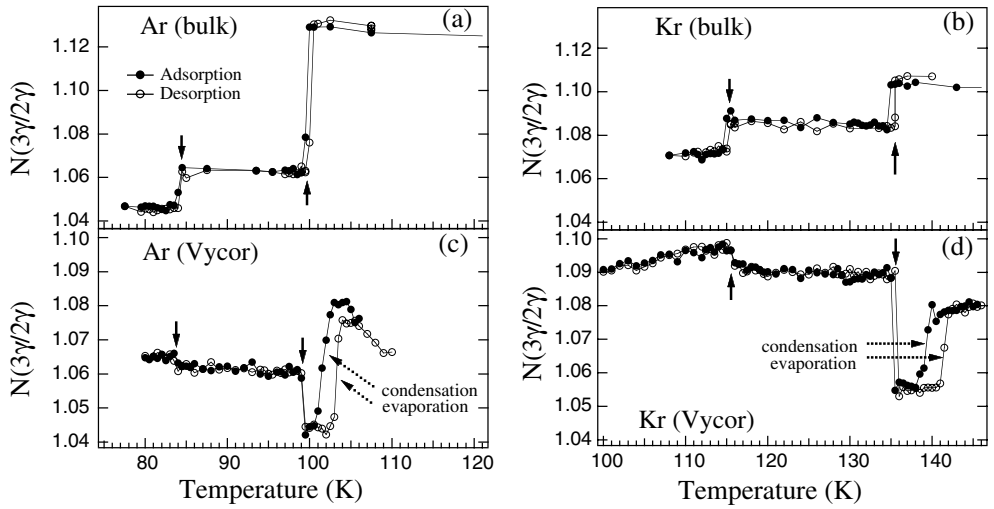

Figure 1. Isobaric data for argon and krypton at a constant pressure of 3 bar. (a) Argon and (b) krypton bulk isobars. The bulk gas/liquid and liquid/solid transitions are indicated by solid arrows. (c) Argon and (d) krypton isobars absorbed in Vycor glass. Bulk transitions occur at the same temperatures as in previous panels. The gas/liquid transitions in the pores (broken arrows) are shifted to higher temperature compared to the case for the bulk and they show significant hysteresis.

were performed to probe the fluid as it filled and emptied from the pores at the gas/liquid phase boundary. The phase behaviour was monitored via the energy spectra of the annihilation photons. The spectra were analysed using two parameters. The N-parameter, $N(3\gamma/2\gamma)$, is defined as the total counts in the range 341–490 keV (3γ) divided by the total counts in the range 490–540 keV (2γ). Although $N(3\gamma/2\gamma)$ does not give an exact balance of the 3γ (oPs) to 2γ (pPs and free positron) annihilation, it is sensitive to variations in these annihilation modes. The second parameter is the S-parameter or 'shape' parameter, which characterizes the shape of the 511 keV annihilation peak. It is defined as the total counts in a narrow window about the 511 keV peak (510.25–511.75 keV) divided by a broader 2γ window (507–515 keV). This normalized parameter largely focuses on the balance of pPs and free positron annihilation. The two parameters are complementary and a joint analysis of them is usually sufficient to monitor all the phase boundaries of interest.

4. Results and discussion

To show the essential features of the various phase transitions, in figure 1 we present two bulk isobars for (a) argon and (b) krypton in terms of $N(3\gamma/2\gamma)$ as a function of decreasing (●) and increasing (○) temperature, at a constant pressure of 3 bar (lying above the bulk triple point). In figure 1(a), starting at high temperature, we observe a step-wise decrease in $N(3\gamma/2\gamma)$ at ∼100 and 84 K coinciding with the argon bulk condensation and freezing transitions, respectively [12]. For krypton (figure 1(b)) the bulk condensation and freezing transitions occur at 135 and 115 K respectively. These results are similar to those from earlier positron work on bulk CO_2 [13] and indicate an increase in oPs quenching on condensation and an inhibition of Ps formation on freezing. It is interesting to note the higher level of oPs (3γ) in liquid and solid krypton compared to argon. Positron angular correlation experiments find a much larger Ps fraction in liquid Kr (32.8%) compared to liquid Ar (26.4%) [11]. It was

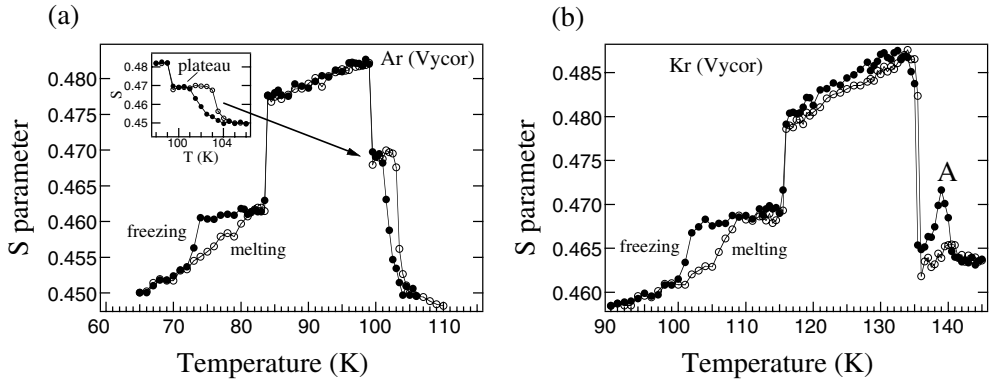

Figure 2. Isobaric data for (a) argon and (b) krypton adsorbed in Vycor and analysed via the *S*-parameter. The pore freezing and melting transitions now become apparent. A peak (A) is seen when krypton condenses in the pores but is absent for argon.

suggested that the increase in Ps formation for the heavier noble gas reflects an accompanying reduction in electron binding energy. The Ps atom exists in a bubble state inside the liquid. Smaller Ps fractions (∼3%) have been measured in solid Ar but there the Ps is not thought to exist in bubbles, but rather is associated with large defects in the material [14].

If the fluids are now adsorbed in the narrow pores of Vycor glass we can see the broad, shifted pore transitions (figures 1(c), (d)). Pore condensation occurs ∼2 K (argon) and ∼4 K (krypton) above the bulk condensation transitions, and there is a hysteresis of ∼2 K in both cases. The bulk transitions (solid arrows) are still seen because of the narrow gap between the positron source and the samples. The Vycor data show some unusual features, which deserve explanation. Condensation of the fluid in the gap leads to an increase in $N(3\gamma/2\gamma)$. This rise is to be expected as more positrons stop in the gap and form Ps (probably in the form of bubbles) when the vapour there condenses to a liquid [13, 15]. However, we also see a similar, but smaller increase as the bulk fluid freezes, indicating some mechanism whereby the solid argon or krypton in the gap supports a larger fraction of oPs than the liquid. The origins of this are unclear but it most likely reflects the close proximity of this bulk frozen material to the Vycor glass and the diffusion of material to and from this environment. The changes in $N(3\gamma/2\gamma)$ as the fluid in the pore condenses or evaporates behave as expected, with increased oPs quenching as the fluid liquefies.

We see no evidence of the fluid freezing or melting in the pores via the $N(3\gamma/2\gamma)$ parameter. However, if we take the same data and analyse the shape of the 511 keV peak in terms of the '*S*'-parameter these transitions become apparent (figure 2). The fluid freezes in the pores at 73 K (argon) and 101 K (krypton), approximately 10 and 15 K below the respective bulk transitions. This difference indicates that the pore wall–fluid interactions are more attractive in the case of argon although in both cases they are only weakly attractive [16]. The hysteresis between freezing and melting is ∼4–6 K and is larger than at the gas/liquid phase boundary. Argon melts in a more continuous way than krypton with no well-defined sharp transition. Similar effects have been seen in studies of pure argon and krypton monolayers physisorbed onto graphite surfaces [17]. Krypton monolayers do not show such behaviour.

The *S*-parameter also highlights a difference between the two gases at the pore condensation transition. An enhanced signature of pPs (peak A) is seen during the latter half of the krypton condensation transition. The peak has disappeared by the time the pore condensation transition has finished (according to the $N(3\gamma/2\gamma)$ parameter). Such a signature

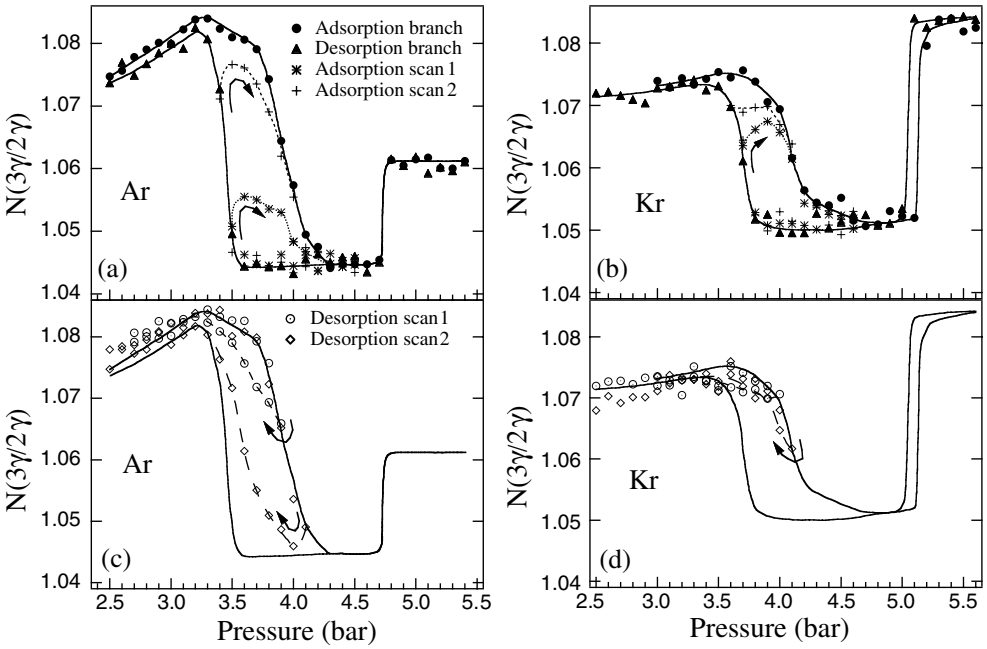

Figure 3. Isothermal scans of argon and krypton absorbed in Vycor glass at a constant temperature of 105 K (Ar) and 145 K (Kr). Adsorption scans for (a) argon and (b) krypton. Desorption scans for (c) argon and (d) krypton.

has been seen before for CO_2 in Vycor [9, 18] and has been attributed to the formation of microbubbles or large gas–liquid interfaces as the pores fill with liquid. We do not see such a feature in argon. Instead the S-parameter rises to a plateau at $\sim$101 K, indicating that the filling mechanism is different there.

We now turn our attention to the gas/liquid phase boundary to explore the pore filling and emptying mechanism in more detail. In this case we decided to probe the phase boundary isothermally. Instead of simply traversing a given adsorption or desorption phase boundary, the pressure was reversed part of the way though the broad pore transition. This 'scanning' process allows us monitor the partially filled and partially empty environment in the pores. These data are summarized in figure 3. Due to the large number of data displayed on these panels, smooth curves have been drawn through the various scans to guide the eye.

The closed symbols and solid curves relate to the full adsorption and desorption branches of the gas/liquid phase boundary. The first thing to note is that the onset of the desorption branch is in general sharper than the onset of the adsorption branch. Such behaviour is expected for the porous network found in Vycor glass where narrow necks lead to a pore blocking effect. Basically, the fluid in the necks evaporates at a lower pressure than the fluid in the larger main pores. It is only once the fluid in the necks evaporates that we get a percolation effect and all the fluid is free to drain quickly away. Now let us consider the adsorption scans ((a) and (b)). Starting from high pressure where all the fluid is liquefied (in both pore and bulk), we reduce the pressure and first cross the bulk liquid–gas transition where $N(3\gamma/2\gamma)$ drops sharply. Reducing the pressure further, we partially cross the desorption branch before increasing the pressure to give an adsorption scan loop. This process partially empties the pores of fluid. As the pores refill it is clear that we must return almost to the main adsorption branch before the fluid recondenses, hence the fluid must have free access to the external bulk fluid reservoir

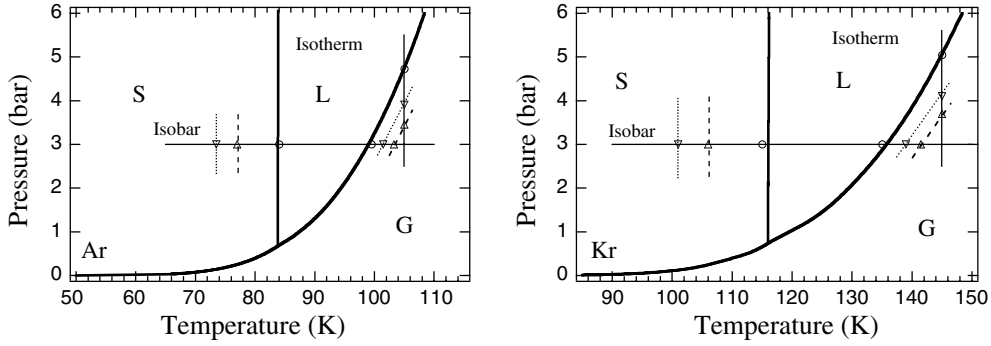

Figure 4. Phase diagrams for argon and krypton. Thick solid lines correspond to previously determined phase boundaries separating the bulk solid (S), liquid (L) and gaseous (G) phases [10]. The thin solid lines trace the isothermal and isobaric range of temperatures and pressures used in our experiment. ○, ▽, △ refer to our determination the bulk, adsorption and desorption phase boundaries, respectively.

and adsorption proceeds according to the original main adsorption branch. This effect is seen in both argon and krypton. At the point where the pressure is reversed it appears that the fluid moves around inside the pores as manifested by the initial rise in $N(3\gamma/2\gamma)$. It is possible that the liquid/vapour mixture diffuses through the pores as the pressure is increased, allowing small vapour regions to coalesce into large bubbles within the porous medium. These larger bubbles support more oPs (3γ) annihilation.

The desorption scans ((c) and (d)) are quite different. Starting from low pressure in the gaseous phase and increasing the pressure we partially cross the adsorption branch then reduce the pressure. This is a partial filling process. When the pressure is reversed the $N(3\gamma/2\gamma)$ parameter recovers much more quickly to the original high level in the gaseous state. Essentially we have removed the pore blocking effect and the curves (especially those where the turning point is at high pressure) most closely resemble the main desorption branch that would be obtained in the absence of a pore blocking effect.

By taking the mid-point of each of the phase boundaries in figures 1–3 we can begin to map out the experimental adsorption and desorption phase diagrams for argon and krypton. This information is summarized in figure 4. Looking at these phase diagrams we can see that the adsorption (dotted lines) and desorption (dashed lines) are shifted by several degrees with respect to the bulk data (thick solid lines). All the shifts are more pronounced for krypton.

In conclusion, the phase behaviour of argon and krypton adsorbed in Vycor glass at pressures somewhat above the bulk triple point display interesting features. We find that the positron technique is sensitive to all the phase boundaries studied. The pore phase boundaries are shifted with respect to bulk and show significant hysteresis. The effects are more pronounced in krypton and probably reflect a less attractive interaction between the fluid and pore walls for that material. The pore filling and emptying processes at the gas/liquid boundary are quite different, with clear evidence of pore blocking on desorption. In addition, microbubbles or large gas–liquid interfaces are postulated to arise during the filling process in krypton and are absent in the case of argon. Finally, the melting process in argon is more continuous than that in krypton.

Acknowledgment

This work was supported by the EPSRC (grant number GR/R19786/01).

References

[1] Elmer T H 1992 Porous and reconstructed glasses *Engineered Materials Handbook: Ceramic and Glasses* vol 4 (Materials Park, OH: ASM International) p 427
[2] Everett D H 1967 *The Solid–Gas Interface* vol 2, ed A Flood (New York: Dekker) p 1055
[3] Gregg S J and Sing K S W 1982 *Adsorption, Surface Area and Porosity* (New York: Academic)
[4] Evans R 1990 *J. Phys.: Condens. Matter* **2** 8989
[5] Lev B G, Gubbins K E, Radhakrishnan R and Sliwinska-Bartkowiak M 1999 *Rep. Prog. Phys.* **62** 1573
[6] Moltz E, Wong A P Y, Chan M H and Beamish J R 1993 *Phys. Rev.* B **48** 5741
Thommes M, Köhn R and Fröba M 2000 *J. Phys. Chem.* B **104** 7932
Thommes M, Köhn R and Fröba M 2000 *Stud. Surf. Sci. Catal.* **128** 259
[7] Li J C, Ross D K and Benham M J 1991 *J. Appl. Crystallogr.* **24** 794
[8] Huber P, Wallacher D and Knorr K 1999 *Phys. Rev.* B **60** 12666
[9] Alam M A, Fretwell H M, Duffy J A, Clarke A P and Dugdale S B 1996 *J. Radioanal. Nucl. Chem.* **210** 255
[10] Ferrell R A 1957 *Phys. Rev.* **108** 167
[11] Varlashkin P G 1971 *Phys. Rev.* A **3** 1230
[12] Cook G A (ed) 1961 *Argon, Helium and Rare Gases* vol 1 (New York: Interscience)
Linstrom P J and Mallard W G (ed) 2001 *NIST Chemistry WebBook (NIST Standard Reference Database Number 69, July 2001)* (Gaithersburg, MD: National Institute of Standards and Technology) p 20899 (http://webbook.nist.gov)
[13] Duffy J A, Wilkinson N J, Fretwell H M and Alam M A 1995 *J. Phys.: Condens. Matter* **7** L27
[14] Stewart A T, Briscoe C V and Steinbacher J J 1990 *Can. J. Phys.* **68** 1362
[15] Duffy J A, Wilkinson N J, Fretwell H M, Alam M A and Evans R 1995 *J. Phys.: Condens. Matter* **7** L713
[16] Dominguez H, Allen M P and Evans R 1999 *Mol. Phys.* **96** 209
[17] Roth M W 1999 *Langmuir* **15** 2169 and references therein
[18] Wilkinson N J, Duffy J A, Fretwell H M and Alam M A 1995 *Phys. Lett.* A **204** 285